THE JOURNAL OF BIOLOGICAL CHEMISTRY
Vol. 280, No. 4, Issue of January 28, pp. 2682–2690, 2005
Printed in U.S.A.

Supramolecular Amyloid-like Assembly of the Polypeptide Sequence Coded by Exon 30 of Human Tropoelastin*

Received for publication, October 12, 2004
Published, JBC Papers in Press, November 18, 2004, DOI 10.1074/jbc.M411617200

Antonio Mario Tamburro‡§, Antonietta Pepe‡, Brigida Bochicchio‡, Daniela Quaglino¶, and Ivonne Pasquali Ronchetti¶

From the ‡Department of Chemistry, Università della Basilicata, Via N. Sauro 85, 85100 Potenza, Italy and the ¶Department of Biomedical Sciences, Università di Modena e Reggio Emilia, Via Campi 287, 41100 Modena, Italy

Elastin is known to self-aggregate in twisted-rope filaments. However, an ultrastructural organization different from the fibrils typical of elastin, but rather similar to those shown by amyloid networks, is shown by the polypeptide sequence encoded by exon 30 of human tropoelastin. To better understand the molecular properties of this sequence to give amyloid fibers, we used CD, NMR, and FTIR (Fourier transform infrared spectroscopy) to identify the structural characteristics of the peptide. In this study, we have demonstrated, by FTIR, that antiparallel β-sheet conformation is predominant in the exon 30 fibers. These physical-chemical studies were combined with transmission electron microscopy and atomic force microscopy to analyze the supramolecular structure of the self-assembled aggregate. These studies show the presence of fibrils that interact side-by-side probably originating from an extensive self-interaction of elemental cross β-structures. Similar sequences, of the general type *X*GG*Z*G (*X*, *Z* = V, L, A, I), are widely found in many proteins such as collagens IV and XVII, major prion protein precursor, amyloid β A4 precursor protein-binding family, etc., thus suggesting that this sequence could be involved in contributing to the self-assembly of amyloid fibers even in other proteins.

Elastin is the protein responsible for the elasticity of skin, arteries, and lung whose elastic properties and resilience depend on its supramolecular organization and cross-linking into fibers and lamellae (1–4). Although, the ability of the elastin precursor molecule to undergo self-aggregation is an important property of the assembly process, the steps involved in elastic fiber formation are not precisely known (5). Actually, it has been widely demonstrated that even short peptides and simple polymeric sequences belonging to elastin are able to give filaments with twisted-rope, hierarchical supramolecular organization similar to that found for the entire protein (6, 7). Interestingly, Miao *et al.* (8) have found that some mutated polypeptide sequences encoded by exons of human tropoelastin exhibit an ultrastructural organization different from the fibrils typical of elastin but rather similar to those found for amyloid networks, constituted by helical fibrils several microns long and about 10 nm wide (9). Recently, Kozel *et al.* (10) have demonstrated that a polypeptide consisting of the sequence coded by exon 30 of bovine tropoelastin formed amyloid-like fibrils.

The fibrous structures referred to as amyloids are widely found (11–13) and are responsible for various medical disorders, *e.g.* bovine spongiform encephalopathies or Creuzfeld-Jacob disease, Alzheimer disease, type II diabetes, or Huntington disease (14).

From a structural point of view, amyloid fibrils contain significant amounts of the cross-β structural motif originally revealed by x-ray diffraction (9). According to current opinion (see, however, Ref. 15), the cross-β-structure originates antiparallel β-sheets extending over the length of the fibril, formed by β-strands that run nearly perpendicular to the long axis of the fibril. Interestingly, β-strands, whose role in elastin assembly has to be ascertained, have been detected in elastin in the solid state (16–18).

Recently, we found that the sequence encoded by exon 30 (EX30)[1] of human tropoelastin is the only sequence in the molecule whose CD spectra roughly resemble a β-sheet conformation (19) and that the conformation of EX30 peptide is temperature- and concentration-dependent (20).

Currently, the criteria to be adopted to assess the presence of amyloid fibrils are quite controversial. On summarizing, positive results for Congo Red binding together with the presence of β-sheet secondary structure revealed by FTIR and/or CD and NMR spectroscopy could be considered sufficient evidences for the presence of amyloid fibers (21). Accordingly, to better understand the molecular properties of EX30, we used CD, NMR, and FTIR to identify the structural characteristics of the peptide. These physical-chemical studies were combined with transmission electron microscopy and atomic force microscopy to analyze the supramolecular structure of the self-assembled aggregate. Our results suggest that the peculiar propensity of EX30 peptide to adopt a β-sheet conformation is the crucial element that favors the adoption of amyloid-like organization.

MATERIALS AND METHODS

CD Spectroscopy—CD spectra for the peptides were obtained using a Jasco J-600 Spectropolarimeter at various temperatures and at concentrations of 0.1 and 1.0 mg/ml in water by using cells of 0.1 and 0.01 cm, respectively. Spectra were acquired in the range 190–250 nm at a temperature of 25 °C by taking points every 0.1 nm, with 20 nm min^{-1} scan rate, an integration time of 2 s, and a 1 nm bandwidth. The data are expressed in terms of [Θ], the molar ellipticity in units of degree cm^2 $dmol^{-1}$.

Nuclear Magnetic Resonance Spectroscopy—All ^1H NMR experiments were performed on a Varian Unity INOVA 500 MHz spectrometer equipped with a 5-mm triple-resonance probe and *z*-axial gradi-

* This work was supported by Grant QLK6-CT-2001-00332 from the European Community and by a COFIN 2002 Grant from Ministero dell'Istruzione, dell'Università e della Ricerca. The costs of publication of this article were defrayed in part by the payment of page charges. This article must therefore be hereby marked "*advertisement*" in accordance with 18 U.S.C. Section 1734 solely to indicate this fact.

§ To whom correspondence should be addressed. Tel.: 39-0971-202242; Fax: 39-0971-202223; E-mail: tamburro@unibas.it.

[1] The abbreviations used are: EX30, exon 30; FTIR, Fourier transform infrared spectroscopy; TFE-d_3, deuterated trifluoroethanol; NOE, nuclear Overhauser effect; PPII, polyproline II.

ents. The purified peptides were dissolved in 700 μl of H_2O/D_2O (90/10) or TFE-d_3/H_2O (80/20), containing 0.1 mM 3-(trimethylsily1)-1-propane sulfonic acid as internal reference standard at 0 ppm. Usually 1.5 mM peptide solutions were used. The ^{1}H NMR spectra were acquired at 15°, 25° and 45 °C in TFE and also at 15 and 25 °C in water. One-dimensional spectra were acquired in Fourier mode with quadrature detection, and the water signal was suppressed by a 2.5-s presaturation pulse. Two-dimensional TOCSY (22) and NOESY (23) spectra were collected in the phase-sensitive mode using the States method (24). Typical data were 2048 complex data points, 8 or 32 transients and 256 increments. Relaxation delays were set to 2.5 s, and spinlock (MLEV-17) mixing time was 80 ms for TOCSY, while 150–250 ms mixing time was applied to NOESY experiments. Shifted sine bell squared weighting and zero filling to 2048 × 2048 was applied before Fourier transformation. The residual HDO signal was suppressed by presaturation for TOCSY, while WATERGATE pulse sequence was used for NOESY experiments (25). Amide proton temperature coefficients were usually measured from one-dimensional ^{1}H NMR spectra recorded in 5 °C increments from 20 to 45 °C; for overlapping resonances a series of TOCSY were recorded to measure the amide temperature coefficients. Spectra were processed and analyzed by VNMR Version 6.1C software (Varian, Palo Alto, CA).

Resonance Assignments of Elastin Peptide—The EX30 peptide was analyzed by ^{1}H NMR spectroscopy in water (H_2O/D_2O 90/10) and mixed aqueous/organic solution (TFE-d_3/H_2O 80/20) at 25 °C. The resonance assignment of the ^{1}H NMR spectra was made by standard sequential assignment procedures (26) and accomplished by a combined analysis of two-dimensinoal TOCSY and two-dimensional NOESY spectra. TOCSY spectra were used to identify spin systems, while NOESY spectra permitted the assignment of resonance to individual amino acids through sequential NOE connectivities. The presence of a considerable number of glycine residues in the peptide sequence (52%) made the assignment of the resonance to the different residues in the sequence difficult. Nevertheless, in TFE-d_3/H_2O solution the complete chemical shift assignments and NOE analysis of the peptide were accomplished. In H_2O/D_2O a stronger degeneracy of the signals precluded the complete NOE analysis of the glycine residues resonance.

The presence of a proline in the EX30 peptide sequence allows cis/trans isomerization to occur in both solution conditions. Nevertheless, we identified only one major conformation (>90%) with all-trans proline conformers. Thus the conformational analysis has been carried out only for the major all-trans peptide molecules.

Congo Red Binding—1.0 ml of a 2 mM solution of the EX30 peptide in Tris (50 mM), NaCl (1.5 M), and $CaCl_2$ (1.0 mM) (pH 7.0) solution was incubated overnight at room temperature. The solution was stirred to suspend the precipitated peptide, and an absorbance spectrum from 400 to 600 nm was collected with a Cary UV spectrophotometer using quartz cuvettes. Congo Red was added to a final concentration of 3.0 M, and the spectrum was recorded.

A third spectrum of the unbound dye was also collected. The spectrum of peptide alone was subtracted from the spectrum of Congo Red with peptide to correct for the turbidity of the sample due to the precipitated material.

FTIR Spectroscopy—EX30 peptide was analyzed by FTIR either as a lyophilized powder or as precipitated fibers in KBr pellets. The spectra were recorded on a Jasco spectrometer using a resolution of 4 cm^{-1} and then smoothed by using the Savintky-Goolay algorithm. The samples were examined at the solid state in KBr pellets (1 mg/100 mg). The decomposition of FTIR spectra was obtained using GRAMS32 software. The percentage of Gaussian and Lorentzian functions was fixed at the 8:2 ratio.

Electron Microscopy—EX30 peptide (1 mg/ml) was solubilized in Tyrode's physiological solution pH 7.2 at room temperature and incubated at 20, 35, and 50 °C for times from 1 up to 48 h. At fixed intervals, 10 μl of the solution were (*a*) placed on Formvar and carbon-coated copper grids, negatively stained with a few drops of 1% uranyl acetate in bidistilled water, air-dried, and observed by transmission electron microscopy and (*b*) spread on freshly cleaved mica, rotary-shadowed with platinum-carbon from an angle of 11 degrees, and covered by evaporated carbon. The replica was floated on bidistilled water, collected on copper grids, air-dried, and observed under the electron microscope.

Atomic Force Microscopy—About 10 μl of the peptide solutions were spread on freshly cleaved mica as described above and salts removed by washing the specimens with twice-distilled water. Samples were stored sealed in a Petri dish until observed by the scanning force microscope (Park Autoprobe). Specimens were observed at room temperature and by the tapping mode.

TABLE I
Alignment of exon 30 coded domains of different tropoelastins

Sequence	Origin
GL--VGAAGLGGLG-VGGLG-VPGVGGLG	Human
GL---G--GVGGLG-VGGLGAVPGAVGLG	Bovine
G---VG--GVGGLG-VGGLGAVPGAGAFG	Porcine
GLGGVGGLGVGGLGAVGGLGAVPGAVGLG	Ovine
* * *:**** ***** *** :*	

RESULTS

Sequence Analysis—The sequence of EX30 peptide is GLVGAAGLGGLGVGGLGVPGVGGLG. In the alternate succession of hydrophobic and cross-linking domains, peculiar of tropoelastin (27), this peptide belongs to the C-terminal hydrophobic domains of human tropoelastin and has been indicated as fundamental for a correct assembly of elastin (10). It is a glycine-rich domain, containing 13 glycine residues up to 25 residues, and contains only hydrophobic residues. A certain homology is evident among sequences of human, bovine, porcine, and ovine tropoelastin (Table I), while in other mammalian, such as in mouse, the EX30-coded domain is constituted by a nine time-repeated pentamer LGAGG. At variance with other hydrophobic domains of human tropoelastin it has no tendency to coacervate (28) but forms peptide aggregates with fibrillar structure instead. Similar sequences, of the general type *X*GGZG (*X*, *Z* = V, L, A, I), are widely found in many proteins such as collagens IV and XVII, fibrillin 2 precursor, flagelliform silk protein, major ampullate gland dragline silk protein, major prion protein precursor, lamprin precursor, and in amyloid β A4 precursor protein-binding family, etc.

CD Difference Spectra—CD spectroscopy is a useful tool in identifying the global conformation of a peptide or a protein. It is also helpful in highlighting the conformational changes as a function of environmental changes, such as temperature, solvent, salt, and peptide concentration. The CD spectra of a protein can be assumed to be the linear combination of the spectra of the secondary structural elements, so difference spectra of CD spectra recorded in different conditions should point out the conformational changes involved. CD spectra of EX30 peptide were recorded in different solvents and at different temperatures.

The CD difference spectra of EX30 in water are shown in Fig. 1. The curve obtained by subtracting the spectra at the two extreme temperatures, 70 and 0 °C, shows a maximum at 202 nm and a minimum at 217 nm. This type of curve is typical of a mixture of β-sheet and unordered conformations and indicates the dominance of the β conformation on increasing the temperatures. At lower temperatures the CD spectra clearly indicate the dominance of PPII conformation (20). A similar effect can be obtained by increasing the peptide concentration. In fact, the CD difference spectrum, obtained by subtracting the curve at 0.1 mg/ml to that at 1.0 mg/ml, shows a maximum at 195 nm and a small minimum at 205 nm (Fig. 2). These spectral features can most likely be attributed to a distorted β-sheet conformation that gives rise to a spectral blue shift and to a strong decrease in the negative band relative to the standard CD of the β-structure. The decrease in the negative band is suggested to be due to a shift of the ψ dihedral that adopts higher values thereby rendering it markedly less negative (see Fig. 13 in Ref. 29).

NMR Spectroscopy—The EX30 peptide has been analyzed in H_2O/D_2O 90/10 and in less polar solvent conditions (TFE-d_3/H_2O 70/30), which better mimic the highly hydrophobic microenvironment of the peptide sequences when inserted in the whole protein.

Several NMR parameters were used to deduce the secondary

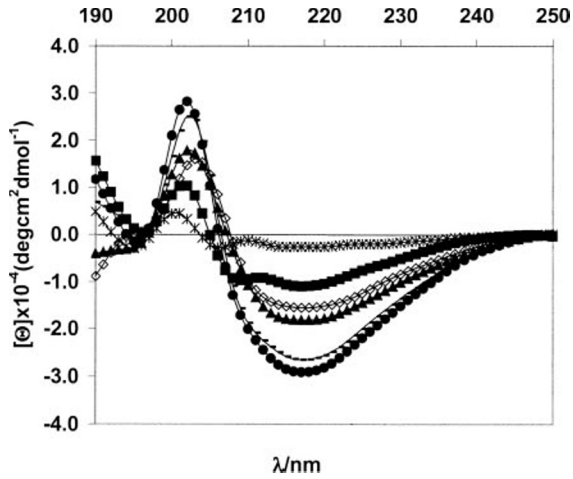

FIG. 1. **CD difference spectra in aqueous solution of EX30 peptide.** ■, 20 °C to 0 °C; ●, 70 °C to 0 °C; —, 60 °C to 0 °C; ◇, 60 °C to 20 °C; ▲, 70 °C to 20 °C; *, 70 °C to 60 °C.

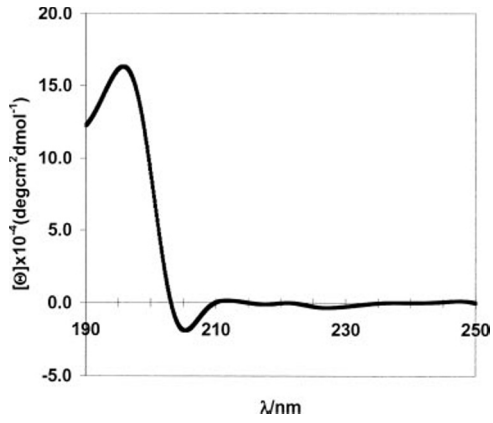

FIG. 2. **CD difference spectrum in aqueous solution of EX30 peptide at 20 °C.** The difference spectrum was obtained by subtracting the curve at 0.1 mg/ml to that at 1 mg/ml.

structure of EX30 peptide: chemical shift index, temperature coefficients of amide chemical shifts, $^3J_{(HN\text{-}H\alpha)}$ coupling constants and the pattern of intra- and inter-residue NOEs.

Chemical shift index analysis (30) is based on the observation that some secondary structures present chemical shifts for some atoms (Hα, Cα, C′), which deviate significantly, from random coil values. In particular, in ^{1}H NMR spectroscopy, chemical shift index is a valuable tool for identifying α-helix and β-sheet simply by comparing the chemical shifts of Hα protons of the residues with the tabulated random coil values. The Hα protons of the EX30 peptide residues show chemical shifts in the range of random coil values, thus excluding the presence of α-helix as well as of β-sheet conformations in both solution conditions. Only Val^{18} exhibited a down-field shift, as expected for residues preceding a proline (30). Furthermore, the absence of typical medium and long range NOE patterns excluded the presence of either α-helix or β-sheet in EX30 in water and TFE solutions.

To investigate the presence of other kind of folded conformations (β-turns, γ-turns) important support came from other NMR parameters such as low temperature coefficients and specific NOEs connectivity. The occurrence of low temperature coefficients ($<4.0 \times 10^{-3}$ ppm K^{-1}) for the amide protons have been attributed to hydrogen bonding of the amide proton to the peptide backbone (31). In the case of β-turns the lowered temperature coefficient is due to the presence of a hydrogen bond between the NH of residue $i+3$ of the turn with the C=O of residue i. A value for the temperature coefficient in the range of 4.0–5.0 is usually attributed to a very weak H-bond or to an equilibrium between turn and other conformations without an H-bond (32). In H_2O/D_2O the EX30 peptide shows, for non-overlapping residues, very high (>7.5 ppb/K) temperature coefficients, thus excluding the presence of H-bonds. For EX30 peptide in TFE solution, some relatively low amide proton temperature coefficients ($4.0 < -\delta\Delta/\delta T < 5.0$) were measured for residues Leu^2, Leu^8, Gly^{15}, Val^{21}, and Gly^{23}, suggesting the presence of some turn conformations (Fig. 3*A*). These were further confirmed by the presence of typical $\delta_{\alpha N}(i,i+2)$ NOE connectivities. The existence of this typical medium range NOE is a good indication of a significant population of turn conformations present in solution (33). In TFE, the occurrence of $\delta_{\alpha N}(i,i+2)$ NOE connectivities between Ala^6/Leu^8, Val^{13}/Gly^{15}, Pro^{19}/Val^{21}, and Val^{21}/Gly^{23}, together with strong $\delta_{NN}(i,i+1)$ NOE connectivities point to the existence of different turn structures in rapid inter-conversion with open conformations (Fig. 3*A*). In water the EX30 peptide shows only intra-residue and sequential NOE connectivities, suggesting the presence of only extended conformations (data not shown). The assignment of extended conformations is also consistent with the weak intraresidue $\delta_{\alpha N}$ NOEs observed, compared with the strong NOE of sequential $\delta_{\alpha N}(i,i+1)$ protons (Fig. 3*B*, *top*) (34). The reduced intensity of δ_{NN} sequential NOE cross-peaks is also typical of extended conformations (Fig. 3*B*, *bottom*). Distinguishing between the two extended conformations, PPII and β-strands, by NMR spectroscopy is not straightforward. PPII and β-strand both belong to the upper left corner of the Ramachandran map, with small differences in their dihedral angles (PPII, $\varphi = -78$, $\psi = 150$; β-strand, $\varphi = -120$, $\psi = 113$). The torsion angles ψ and φ are essential parameters for defining the backbone conformation of a polypeptide chain. Among these, the φ angle can be evaluated by measuring the $^3J_{(HN\text{-}H\alpha)}$ coupling constants, to which this angle is related. The $^3J_{(HN\text{-}H\alpha)}$ coupling constants were measured from the one-dimensional spectra, and the extracted values were used for calculating dihedral angle φ, applying the Karplus equation (35) as parameterized by Vuister and Bax (36). While this NMR parameter is particularly useful in the case of highly stable and regular secondary structures such as α-helix and β-sheet, it is less informative in the case of flexible and not regular peptides (37). Values for $^3J_{(HN\text{-}H\alpha)}$ between 6 and 7.5 Hz are usually attributed to random conformations or PPII conformations, while values above 8 Hz are usually considered strong indication of β-strand. Nevertheless where the $^3J_{(HN\text{-}H\alpha)}$ coupling constant could be measured, values were generally found to be larger than the random coil values. This trend toward higher values was more pronounced when the temperature was increased, pointing to a thermal transition toward the β-strand conformation, as was also suggested by CD difference spectra.

FTIR Spectra—The deconvoluted FTIR spectrum of the amide I and II regions of lyophilized EX30 peptide is shown in Fig. 4. The amide I region contains two main components at 1671 cm^{-1} and at 1651 cm^{-1}. The first one is usually assigned to non-hydrogen-bonded groups or groups weakly bonded to the solvent, normally absorbing at 1666 to 1670 cm^{-1} (38). In our case, because of the absence of the solvent, the band is essentially due to the presence of PPII conformation (39, 40), which is an extended structure lacking intramolecular hydrogen bonds (20, 29). Furthermore, the component at 1651 cm^{-1} is assigned to unordered conformations and/or α-helical conformations (41). The amide I region also presents two small bands at 1633 cm^{-1} and at 1693 cm^{-1} indicative of cross-β and antiparallel β-sheet structures, respectively (42–44). We propose for the EX30 lyophilized peptide a dominance of PPII conformation together with unordered structures, with β-structures

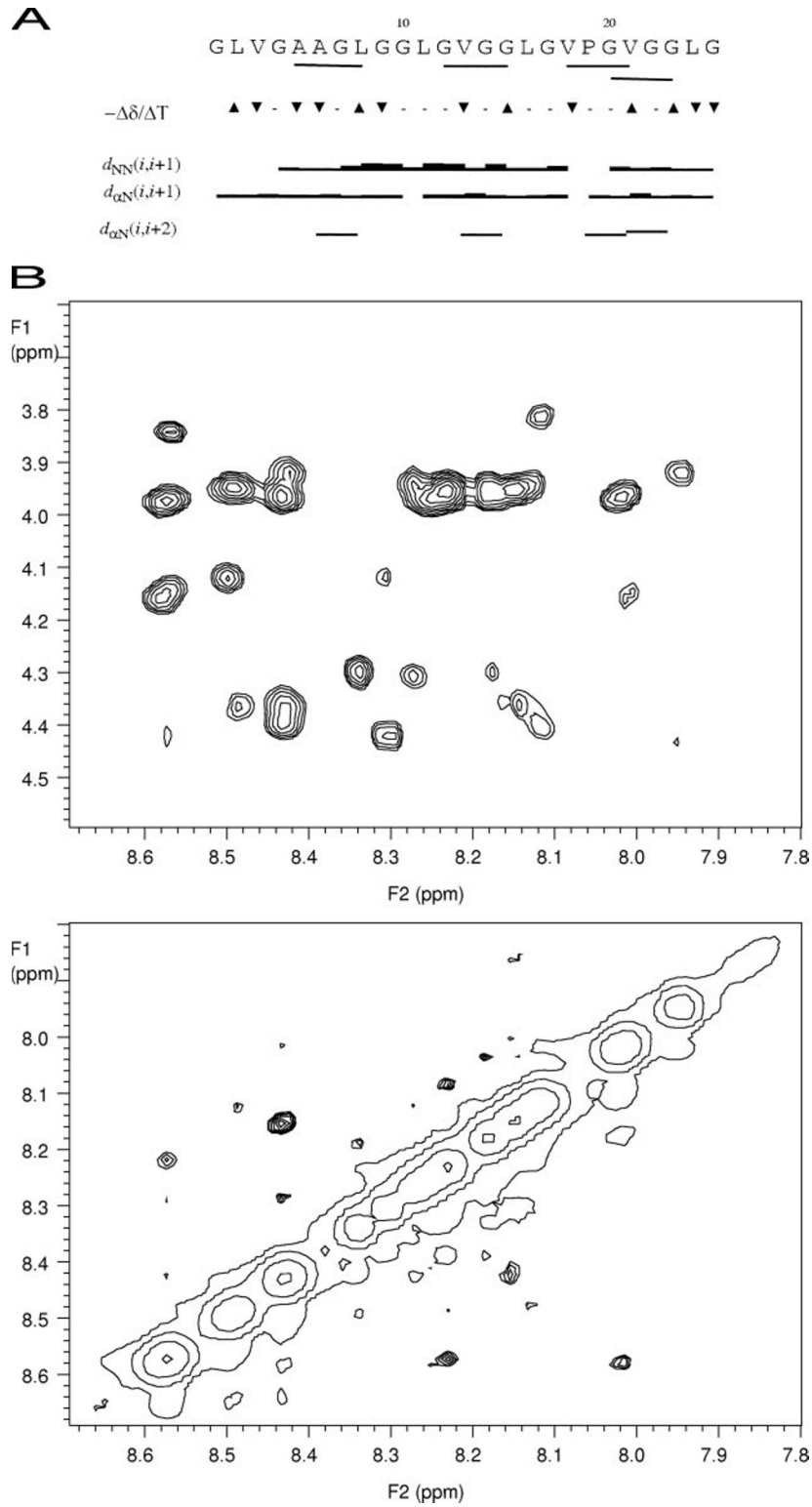

FIG. 3. *A*, summary of the NMR parameters of EX30 peptide in TFE-d3/H2O (80/20) at 289 K. The *underlined* residues of the sequences represent those involved in β-turns. The summary includes the temperature coefficients ($-\Delta\delta/\Delta T$, ppb/K; ▲, >5 ppb/K; ▼, <5 ppb/K) and sequential and medium range NOEs. The NOE intensities are reflected by the thickness of the line. *B*, the fingerprint region and the amide region of the ROESY spectra of EX30 peptide recorded in H_2O/D_2O (90/10) at 298 K. The regions where displayed with the same threshold, to highlight the difference in intensity of the cross-peaks.

being of minor contribution. This interpretation is supported by the appearance of the band at 1549 cm^{-1} in the amide II (Fig. 4) region, which was attributed to PPII conformation in poly(GGA). This polymer has repeating triplets of the GG*X* type (45) similar to those found in the EX30 sequence. Furthermore, the presence of small amounts of β conformation is confirmed by the band at 1524 cm^{-1}, which is normally attributed to the dominance of the bending of hydrogen bonded NH groups in antiparallel β-sheet structures (46). FTIR analysis of the Amide I region of EX30 fibers (Fig. 5) shows a prominent band at 1629 cm^{-1} due to antiparallel β-sheets of the cross-β type, as assigned above, together with a small band at 1697 cm^{-1}, which is typical of the antiparallel β-sheet conformation. Two minor bands at 1649 and 1673 cm^{-1} could originate from unordered and PPII conformations, respectively. The deconvoluted amide II region of EX30 fibers (Fig. 5) shows two components at 1516 cm^{-1} as well as at 1558 cm^{-1} that are considered representative of the presence of β-sheet conformation (45, 46). The band at 1542 cm^{-1} could be tentatively assigned to the unordered component.

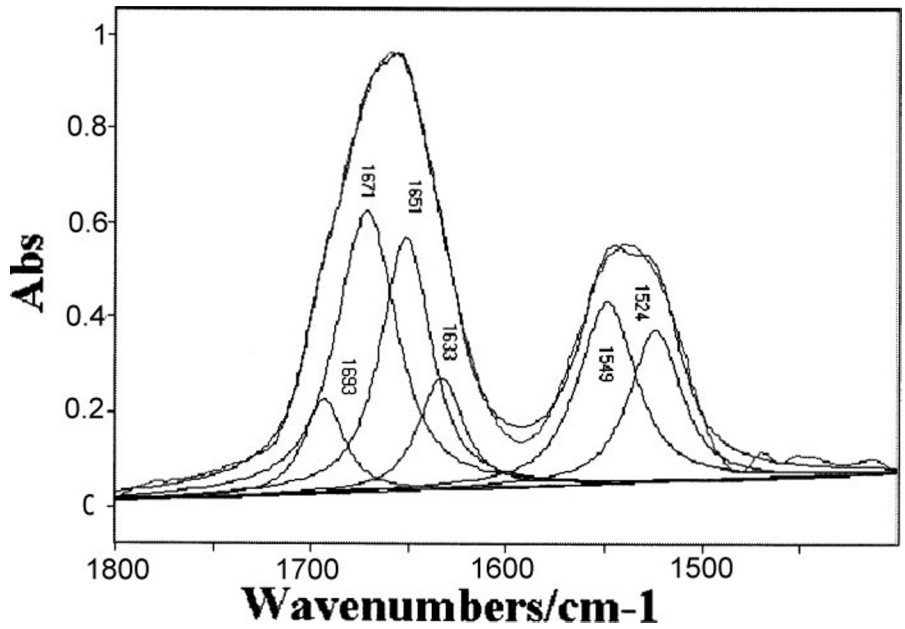

FIG. 4. **FTIR deconvolution spectrum.** Amide I and II regions of liophylized EX30 peptide in KBr pellet.

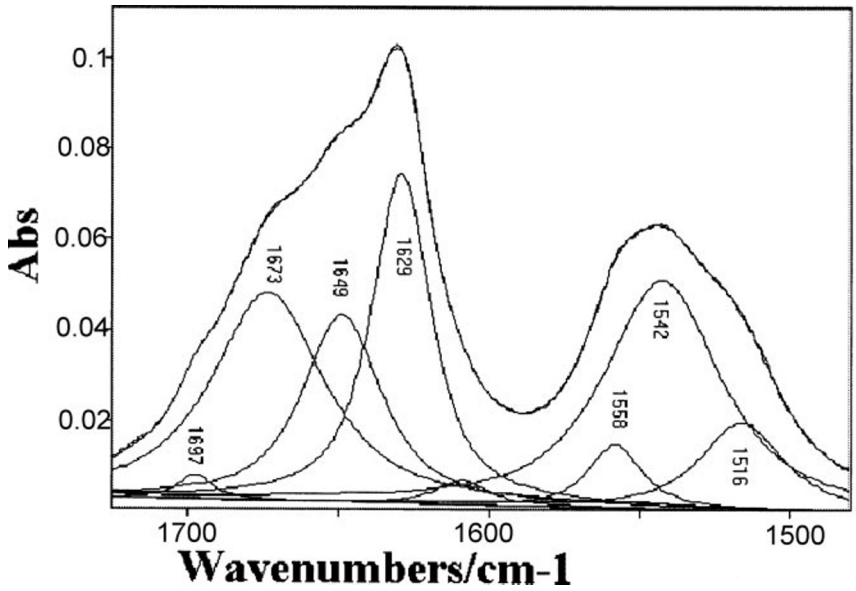

FIG. 5. **FTIR deconvolution spectrum amide I and II regions of EX30 fibers in KBr pellet.**

Together, the FTIR data clearly show that the antiparallel β-sheet is the main structural component of EX30 fibers, whereas in the lyophilized EX30 peptide it is of minor contribution because of the dominance of PPII and unordered conformations. The amide A analysis of both peptides is shown in Figs. 6 and 7. It is evident the presence of one strong band at 3302–3303 cm^{-1}, which is also present in collagen and elastin (47), which both contain the PPII conformation. In addition, it is to be noted that the amide A of lyophilized EX30 shows the presence of significant absorptions originating from the OH stretching of water at 3491 and 3562 cm^{-1}, which are negligible in the case of EX30 fibers. A possible interpretation may lie in the fact that fiber formation is a strongly hydrophobic process giving rise to a sudden segregation of the β-structured polypeptide chains from the aqueous environment. In contrast, lyophilization is a slow process allowing the water inclusion into the polypeptide chains.

Time-dependent Fibril Formation and Congo Red Dye Binding—The *EX30* peptide (1.0 mM) in Tris buffer (50 mM), NaCl (1.5 M), $CaCl_2$ (1 mM) (pH 7.0) solution formed a gel-like material after 12 h at room temperature (Fig. 8). The formation of viscous material is indicative of the formation of amyloid-like fibrils (48, 49). The interaction of this material with Congo Red dye is shown in Fig. 9 and provides additional evidence for the ability of EX30 to self-assemble to form amyloid-like structures. Congo Red is widely used as an indicator of amyloid deposition. The binding interaction is characterized by both hyperchromic (absorbance increase) and bathochromic (red-shift) effects in the absorbance spectrum of the dye (50).

Microscopy Studies—Peptides derived from EX30, solubilized in physiological solution, and warmed up to 50 °C were analyzed by negative staining and rotary shadowing electron microscopy and by scanning force microscopy. After a few minutes incubation at 50 °C, the EX30 peptide formed 20–25-nm-wide globules and 10–12-nm-thick filaments of variable length, which tended to form sheets on the substrate. For incubation times longer than 48 h, the majority of peptides were organized into rather rigid filaments of various length and thickness which had the appearance of twisted ropes (Fig. 10, *a–d*). Their thickness varied from about 20 to 80 nm, and the pitch of the helix varied from 25 to 110 nm depending on the filament thickness.

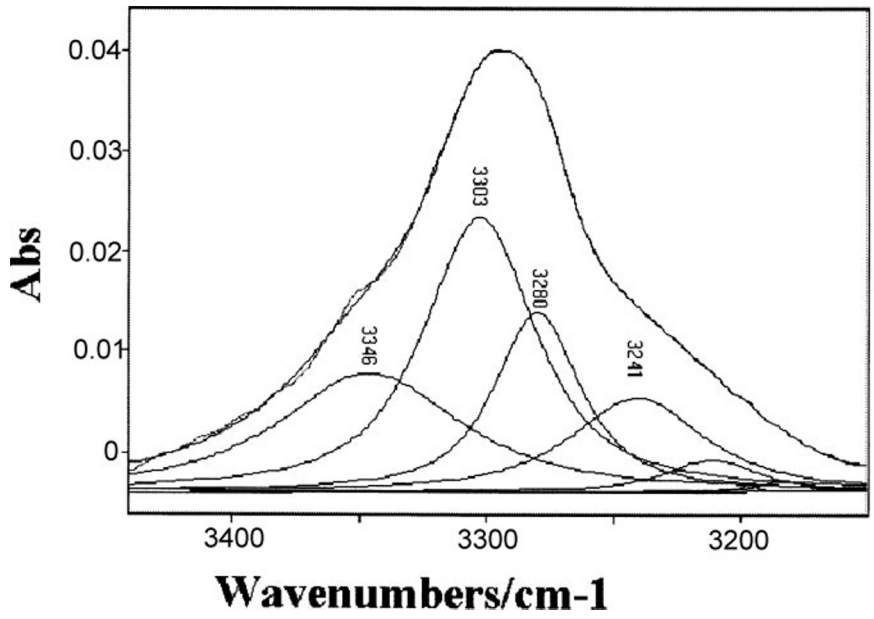

FIG. 6. **FTIR deconvolution spectrum Amide A regions of EX30 peptide in KBr pellet.**

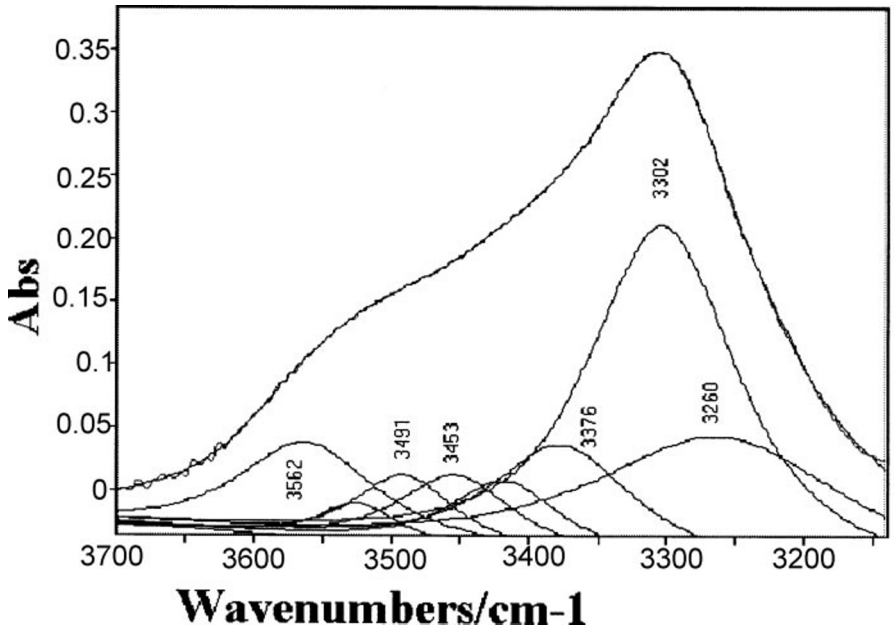

FIG. 7. **FTIR deconvolution spectrum Amide A regions of liophylized EX30 peptide in KBr pellet.**

By scanning force microscopy, these elements revealed a rather complex organization (Fig. 11, *a–f*). Short and rigid filaments were still observed (Fig. 11*a*), which tended to form latero-lateral aggregates (Fig. 11*d*). In Fig. 11*e* a filament segment consisting of three globules can be resolved into a complex set of elements whose organization suggests a precise molecular orientation and ordered interconnections. Fig. 11*f* clearly shows that each filament, about 20 nm thick, consists of discrete elements that form an ordered array and contact similar elements on the adjacent filament, thereby giving rise to a composite filament about 60 nm thick.

DISCUSSION

The results obtained in this study show that the sequence encoded by exon 30 of human tropoelastin is able to give rise to an aggregation process induced by microenvironmental changes such as temperature and time. The end product of the aggregation is the formation of fibrils with an amyloid-like structure.

At the molecular level, the structure adopted by the EX30 peptide is highly dependent on solvent conditions. In TFE, the peptide adopts a folded conformation characterized by several β-turns as suggested by CD. Accordingly, NMR data strongly indicate the presence of turns spanning the sequences ^{5}AAGL^{8}, ^{12}GVGG^{15}, ^{18}VPGV^{21} and ^{20}GVGG^{23}, the last two possibly belonging to the so-called sliding β-turns (51). Differently from TFE, in aqueous solution the peptide is mainly characterized by the presence, possibly in equilibrium, of PPII and β-sheet conformations. The ratio of these structures depends on temperature and/or concentration and time, with the PPII structure being preferred at low temperature (this study) and at low concentration (20) and the β-sheet conformation being favored by opposite conditions.

In addition, FTIR studies in the solid state allowed us to observe the conformational differences of EX30 both as a lyophilized powder and as fibers. The results obtained demonstrate that although the β-sheet and PPII generally appears in both samples, the antiparallel β-sheet conformation is chiefly found in fibers. In the lyophilized powder, PPII and unordered conformations predominate. The presence of antiparallel β-sheet chains, probably originating from cross-β-structures, is

FIG. 8. **Precipitation of EX30 peptide.** EX30 peptide (1.0 mM) in Tris buffer (50 mM), NaCl (1.5 M), and $CaCl_2$ (1 mM) (pH 7.0) formed a gel-like material after 12 h.

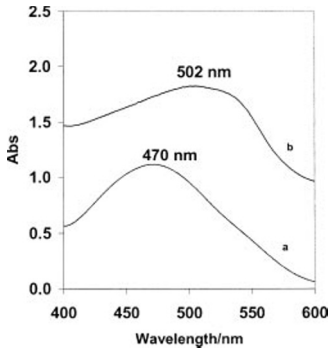

FIG. 9. **Affinity of Congo Red to EX30 at room temperature.** UV absorption spectrum of Congo Red (*curve a*) and of Congo Red bound to EX30 peptide (*curve b*).

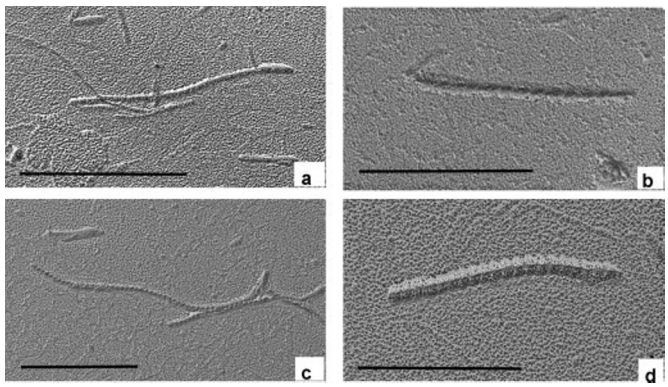

FIG. 10. **TEM micrographies of EX30 peptide.** Observations after rotary shadowing. *Bar*: 1 μm.

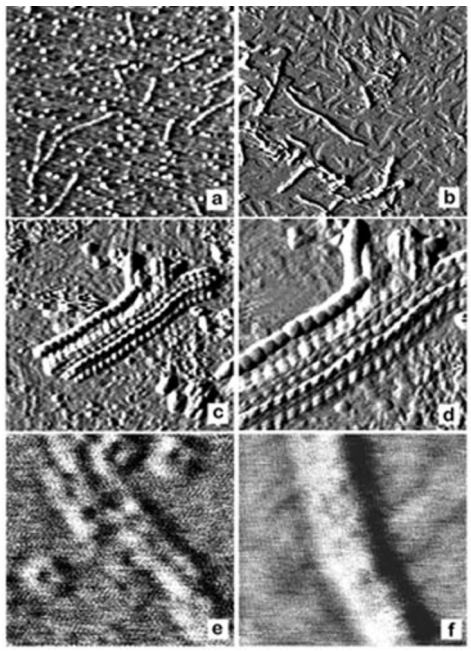

FIG. 11. **AFM of EX30 peptide.**

similar to what was suggested for elastin and lamprin sequences that share the GGLG*X* motif tandem repeat found in the EX30 sequence (52, 53). Different experimental and theoretical studies have indicated in a combination of electrostatic, polar, and hydrophobic interactions the driving force toward amyloid formation (54). The absence of any polar amino acid in the sequence suggests that, in the case of EX30, amyloid fiber formation is predominantly driven by hydrophobic interactions. By increasing the temperature and/or the concentration of the peptide the hydrophobic interactions are favored, thus determining the crucial transition to the β-sheet conformation, strictly related to the aggregated state.

The possibility that the formation of β-structures give rise to aggregation is consistent with the mechanism proposed for the formation of amyloid fibrils by proteins such as lysozyme and transthyretin. Specifically, the formation of fibrils is a consequence of an unfolding process, induced by changes in microenvironment, which leads to antiparallel alignment of cross β-structures that in turn give rise to the formation of fibrils and other aggregates that accumulate in the extracellular space (Ref. 55 and references therein). By contrast, this conformation is almost disfavored by the presence of proline residues that stabilize the PPII structure (29) and whose ϕ dihedral angle is frozen at a value (around $-70°$) not compatible with that of antiparallel β-structure (around $-120°$).

Quite interestingly, an increase of temperature and/or concentration also favors another type of self-aggregation, namely coacervation, although involving different sequences.

Coacervation is one of the peculiar properties of tropoelastin and has been proposed to promote alignment and cross-linking of tropoelastin molecules (56). It is a reversible self-aggregation process in which the protein separates from the solution as a second phase on increasing the temperature. In this case one can observe the formation of well ordered filamentous structures (57), while from a conformational point of view, coacervation promotes the formation of folded conformations, mainly β-turn conformations (58). The domains of human tropoelastin responsible for coacervation have been identified recently (28). Interestingly, these domains all belong to the larger proline-rich domains of tropoelastin (exon 18, exon 20, exon 24, and exon 26 coded domains). Finally, to coacervate the polypeptide sequences should be relatively long and possess a certain number of proline residues.

It has also been observed that polypeptide elastin-like sequences rich in proline, which undergo coacervation, are unable to form amyloid-like fibrils (9). Accordingly, the EX30 peptide gives rise to amyloid fibrils and does not coacervate but precipitates irreversibly (28). Although the role of proline residues in promoting the coacervation seems to be well established, there are polypeptide sequences encoded by the so-called KP domains of human tropoelastin that are unable to coacervate, even though they are rich in proline (data not shown). To this regard, we suggest that the peculiar propensity of isolated EX30 peptide to adopt a β-sheet conformation is the crucial element that favors

the adoption of amyloid-like organization rather than that expected for other elastin-like sequences.

Electron microscopy and atomic force microscopy of EX30 aggregates show the presence of fibrils that interact side by side and that could originate from an extensive self-interaction of elemental cross β-structures. Quite interestingly, the elastin-like biopolymer poly(VGGVG), which comprises the sequences LGGLG and VGGLG similar to those contained in EX30 peptide, has been shown to self-assemble in an amyloid-like pattern when deposited from aqueous suspensions (59). The fibrils did not solubilize after dilution, indicating the irreversibility of the process, also in this case.

Moreover, the sequence VGGLG is repeatedly found also in the prion protein, thus suggesting that this sequence could be involved in contributing to the self-assembly of amyloid fibers even in other proteins.

At this point, a question arises: the propensity of EX30 peptide toward amyloid fiber formation has a biological relevance for elastin and elastic fiber assembly?

Using an *in vitro* elastic fiber assembly system and parallel studies on transgenic mice where tropoelastin constructs were expressed, Kozel *et al.* (10) have evidenced the crucial role of C-terminal domains of tropoelastin for a correct elastic fiber formation. It has been suggested that EX30 domain is the major responsible for the interaction with microfibrils and that this interaction could be mediated by a mechanism of amyloid-like self-aggregation route.

Unquestionably, EX30 coded domain of tropoelastin is crucial for elastic fiber formation, as also indirectly demonstrated by the observation that all the different isoforms of tropoelastin contain it, but the way it happens has to be further investigated.

Our suggestion is that EX30 peptide, when inserted into the protein, does not favor amyloid-like aggregation but rather participates to the formation of filaments and bundles of filaments typical of the elastic fiber. Consistently, Miao *et al.* (8) demonstrated that in a polypeptide sequence constituted by different tropoelastin domain, the substitution of exon 24 domain with exon 30 domain did not alter the coacervation properties. On the contrary, when EX30 peptide is isolated from the protein it leads to the amyloid-like fibril organization reported *in vitro* in the present paper.

Now, we would like to discuss, admittedly in a speculative manner, the possible relevance of these findings to some pathologies that affect elastic tissues (*e.g.* cardiovascular diseases and acute interstitial lung disease).

It is interesting to note that deposition of elastotic material in arteries occurs in aged, atherosclerotic humans,[2] and in lung alveoli in the case of acute interstitial lung disease. In the latter case, the elastotic material was shown to contain amyloid-like fibers (60). Furthermore, it is also known (61) that the degradation of human tropoelastin by elastase is strongly enhanced by the presence of unsaturated fatty acids, the same lipids found to accumulate on elastic fibers in atheromathous plaques. Accordingly, it is tempting to speculate that under certain pathological conditions, EX30-derived soluble peptides released from elastin by proteolytic degradation could slowly aggregate because of mutated microenvironment to form amyloid-like structures that explain the amyloid "elastotic material" described in numerous reports. In fact, peptides PGVGGL and AGLGGLGVGGV, which belong to the EX30 sequence, have recently been identified in an elastase digest of insoluble human elastin (62). Therefore, EX30 peptide could play a role in the development and progression of pathological events that arise secondary to degradation of elastin.

[2] M. Spina, personal communication.

REFERENCES

1. Weinstein, G. D., and Boucek, R. J. (1960) *J. Invest. Dermatol.* **35,** 227–228
2. Varadi, D. P. (1972) *J. Invest. Dermatol.* **59,** 238–246
3. Uitto, J., Paul, J. L., Brockley, K., Pearce, R. H., and Clark, J. G. (1983) *Lab. Invest.* **49,** 499–505
4. Debelle, L., and Tamburro, A. M. (1999) *Int. J. Biochem. Cell Biol.* **31,** 261–272
5. Vrhovski, B., Jensen, S., and Weiss, A.S. (1997) *Eur. J. Biochem.* **250,** 92–98
6. Castiglione Morelli, M. A., De Biasi, M., De Stradis, A., and Tamburro, A. M. (1993) *J. Biomol. Struct. Dyn.* **11,** 181–190
7. Bochicchio, B., Floquet, N., Pepe, A., Alix, A. J. P., and Tamburro, A. M. (2004) *Chem. Eur. J.* **10,** 3166–3176
8. Miao, M., Bellingham, C. M., Stahl, R. J., Sitarz, E. E., Lane, C. J., and Keeley, F. W. (2003) *J. Biol. Chem.* **278,** 48553–48562
9. Tycko, R. (2004) *Curr. Opin. Struct. Biol.* **14,** 96–103
10. Kozel, B. A., Wachi, H., Davis, E. C., and Mecham, R. P. (2003) *J. Biol. Chem.* **278,** 18491–18498
11. Dobson, C. M. (1999) *Trends Biochem. Sci.* **24,** 329–332
12. Kelly, J. W. (1996) *Curr. Opin. Struct. Biol.* **6,** 11–17
13. Chiti, F., Taddei, N., Baroni, F., Capanni, C., Stefani, M., Ramponi, G., and Dobson, C. M. (2002) *Nat. Struct. Biol.* **9,** 137–143
14. Ross, C. A., and Poirier, M. A. (2004) *Nat. Med.* **10,** S10–S17
15. Balbach, J. J., Petkova, A. T., Oyler, N. A., Antzutkin, O. N., Gordon, D. J., Meredith, S. C., and Tycko, R. (2002) *Biophys. J.* **83,** 1205–1216
16. Debelle, L., Alix, A. J. P., Jacob, M. P., Berjot, M., Sombret, B., and Legrand, P. (1995) *J. Biol. Chem.* **270,** 26099–26103
17. Debelle, L., Alix, A. J., Wie, S. M., Jacob, M. P., Huvenne, J. P., Berjot, M., and Legrand, P. (1998) *Eur. J. Biochem.* **258,** 533–539
18. Bochicchio, B., Ait-Ali, A., Tamburro, A. M., and Alix, A. J. (2004) *Biopolymers* **73,** 484–493
19. Tamburro, A. M., Bochicchio, B., and Pepe, A. (2003) *Biochemistry* **42,** 13347–13362
20. Bochicchio, B., and Tamburro, A. M. (2002) *Chirality* **14,** 782–792
21. Nilsson, M. R. (2004) *Methods* **34,** 151–160
22. Braunschweiler, L., and Ernst, R. R. (1983) *J. Magn. Reson.* **53,** 521–528
23. Jeener, J., Meier, B. H., Bachmann, P., and Ernst, R. R. (1979) *J. Chem. Phys.* **71,** 4546–4553
24. States, D. J., Haberkorn, R. A., and Ruben, D. J. (1982) *J. Magn. Reson.* **48,** 286–292
25. Piotto, M., Saudek, V., and Sklenar, V. (1992) *J. Biomol. NMR* **2,** 661–665
26. Wüthrich, K. (1986) *NMR of Proteins and Nucleic Acids*, John Wiley & Sons, Inc., New York
27. Indik, Z., Yeh, H., Ornstein-Goldstein, N., Sheppard, P., Anderson, N., Rosenbloom, J. C., Peltonen, L., and Rosenbloom, J. (1987) *Proc. Natl. Acad. Sci. U. S. A.* **84,** 5680–5684
28. Pepe, A., Guerra, D., Bochicchio, B., Quaglino, D., Pasquali Ronchetti, I., and Tamburro, A. M. (2004) *Matrix Biol.*, in press
29. Woody, R. W. (1992) *Adv. Biophys. Chem.* **2,** 37–79
30. Wishart, D. S., Sykes, B. D., and Richards, F. M. (1992) *Biochemistry* **31,** 1647–1651
31. Dyson, H. J., Rance, M., Houghten, R. A., Lerner, R. A., and Wright, P. E. (1988) *J. Mol. Biol.* **201,** 161–200
32. Tamburro, A. M., Guantieri, V., Scopa, A., and Drabble, J. M. (1991) *Chirality* **3,** 318–323
33. Dyson, H. J., Bolinger, L., Feher, V. A., Osterhout, J. J., Yao, J., and Wright, P. (1998) *Eur. J. Biochem.* **255,** 462–471
34. Fiebig, K. M., Schwalbe, H., Buck, M., Smith, L. J., and Dobson, C. M. (1996) *J. Phys. Chem.* **100,** 2661–2666
35. Karplus, M. (1959) *J. Chem. Phys.* **30,** 11–15
36. Vuister, G. W., and Bax, A. (1993) *J. Am. Chem. Soc.* **115,** 7772–7777
37. Bürgi, R., Pitera, J., and van Gunsteren, W. F. (2001) *J. Biomol. NMR* **19,** 305–320
38. Jackson, M., and Mantsch, H. H. (1991) *Biochim. Biophys. Acta* **1079,** 231–235
39. Martino, M., Bavoso, A., Guantieri, V., Coviello, A., and Tamburro, A. M. (2000) *J. Mol. Struct.* **519,** 173–189
40. Harris, P. I., and Chapman, D. (1995) *Biopolymers* **37,** 251–263
41. Surewicz, W. K., Mantsch, H. H., and Chapman, D. (1993) *Biochemistry* **32,** 389–394
42. Lefèvre., T., Arsenault, K., and Pézolet, M. (2004) *Biopolymers* **73,** 705–715
43. Susi, H., Timasheff, S. N., Stevens, L. J. (1967) *Biol. Chem.* **242,** 5467–5473
44. Clark, A. H, Saunderson, D. H. P., and Suggett, A. (1981) *Int. J. Pept. Protein Res.* **17,** 353–364
45. Andries, J. C., Anderson, J. M., and Walton, A. G. (1971) *Biopolymers* **10,** 1049–1057
46. Bandekar, J. (1992) *Biochim. Biophys. Acta* **1120,** 123–143
47. Debelle, L., and Alix, A. J. P. (1999) *Biochimie* (*Paris*) **81,** 981–994
48. Chiti, F., De Lorenzi, E., Grossi, S., Mangione, P., Giorgetti, S., Cacciolanza, G., Dobson, C. M., Merlini, G., Ramponi. G., and Bellotti, V. (2001) *J. Biol. Chem.* **276,** 46714–46721
49. Zurdo, J., Guijarro, J. L., Jimenez, J. L., Saibil, H. R., and Dobson, C. M. (2001) *J. Mol. Biol.* **311,** 325–340
50. Klunk, W. E., Jacob, R.F., and Mason, R. P. (1999) *Methods Enzymol.* **309,** 285–305
51. Tamburro, A. M., Guantieri, V., Pandolfo, L., and Scopa, A. (1990) *Biopolymers* **29,** 855–870
52. Bochicchio, B., Pepe, A., and Tamburro, A. M. (2001) *Matrix Biol.* **2,** 243–250
53. Robson, P., Wright, G. M., Sitarz, E., Maiti, A., Rawat, M., Youson, J. H., and Keeley, F. W. (1993) *J. Biol. Chem.* **268,** 1440–1447
54. DuBay, K. F., Pawar, A. P., Chiti, F., Zurdo, J., Dobson, C. M., and Vendruscolo, M. (2004) *J. Mol. Biol.* **341,** 1317–1326

55. Petsko, G. A., and Ringe, D. (2004) *Protein Structure and Function* (Lawrence, E., and Robertson, M., eds) New Science Press Ltd., London
56. Bellingham, C. M., Lillie, M. A., Gosline, J. M., Wright, G. M., Starcher, B. C., Bailey, A. J., Woodhouse, K. A., and Keeley, F. W. (2003) *Biopolymers* **70,** 445–455
57. Bressan, G. M., Castellani, I., Giro, M. G., Volpin, D., Fornieri, C., and Pasquali Ronchetti, I. (1983) *J. Ultrastruct. Res.* **82,** 335–340
58. Urry, D. W. (1988) *J. Protein Chem.* **7,** 1–34
59. Flamia, R., Zhdan, P. A, Martino, M., Castle, J. E., and Tamburro, A. M. (2004) *Biomacromolecules* **5,** 1511–1518
60. Fan, K., and Nagle, W. A. (2002) *BMC Pulmonary Medicine* **2,** 5
61. Guantieri, V., Tamburro, A. M., and Daga Gordini, D. (1983) *Connect. Tissue Res.* **12,** 79–83
62. Getie, M., Schmelzer, C., and Neubert, R. H. H. (2004) *Matrix Biol.* **23,** 402